Reprinted from The Journal of Physical Chemistry, 1995, 99.

Structure and Wetting Properties of ω-Alkoxy-*n*-alkanethiolate Monolayers on Gold and Silver[1,2]

Paul E. Laibinis,*,†,‡ Colin D. Bain,*,†,§ Ralph G. Nuzzo,*,⊥ and George M. Whitesides*,†

Department of Chemistry, Harvard University, Cambridge, Massachusetts 02138, Department of Chemical Engineering, Massachusetts Institute of Technology, Cambridge, Massachusetts 02139, Physical Chemical Laboratory, Oxford University, South Parks Road, Oxford, U.K. Ox1 3QZ, and Materials Research Laboratory, Departments of Materials Science and Engineering and Chemistry, University of Illinois at Urbana-Champaign, Urbana, Illinois 61801

Received: August 15, 1994; In Final Form: December 5, 1994[⊗]

ω-Alkoxy-*n*-alkanethiols ($HS(CH_2)_nOR$) adsorb from solution onto the surfaces of evaporated silver and gold films and form oriented self-assembled monolayers (SAMs). For many of these SAMs (R ≥ propyl), the wetting properties of the SAMs by various polar and nonpolar liquids are indistinguishable from those of SAMs derived from *n*-alkanethiols and suggest that the presence of the ether oxygen atom is not sensed by contacting liquids. The structures of the SAMs that form from these adsorbates on silver and gold are different from, but reminiscent of, the canted structures that form upon adsorption of *n*-alkanethiols ($CH_3(CH_2)_xSH$) onto these metal surfaces. The structural differences that exist between the SAMs on the two metals do not affect the wetting properties of the SAMs. The structure of the SAMs on the two metals has been determined using X-ray photoelectron spectroscopy (XPS), reflection absorption infrared spectroscopy (RAIRS), and sum-frequency generation spectroscopy (SFS). Application of these techniques indicates that the ether oxygen atom causes a local disordering and increases the population of gauche conformations. The magnitude of this disordering depends sensitively on the position of the oxygen atom along the chain. When the oxygen atom was located ~2 or more methylene units away from the chain end, the terminal methyl group in the SAMs exhibited the same molecular orientations as is found in SAMs that do not contain the heteroatom. This observation suggests that this type of substitution constitutes a weak perturbation of chain ordering, and one which need not affect the structure of an extended chain.

Introduction

Long chain *n*-alkanethiols ($HS(CH_2)_xX$) are well-known to absorb spontaneously from solution onto gold and silver surfaces and form densely packed, oriented monolayer films (self-assembled monolayers, SAMs).[2-9] The metal−sulfur interaction is sufficiently specific that, on both metals, SAMs can be prepared that have a wide range of polar and nonpolar functionalities positioned at (or close to) the interface between the SAM and the contacting fluid (air or liquid).[5,9-17] This flexibility in synthesis and properties has made SAMs on silver and gold, particularly those derived from substituted alkanethiols ($X \neq CH_3$), useful materials with which to study wetting,[2,9-13] adhesion,[14] nucleation,[15] electron transfer,[16] and X-ray-induced damage.[17] The structures of SAMs on silver and gold derived from *unsubstituted* *n*-alkanethiols have been examined by various techniques and found to be different: on gold, the hydrocarbon chain cants ~30° from the surface normal;[4,8,18-20] on silver, the hydrocarbon chain is oriented closer to the surface normal (cant angle ≤ 13°).[7,8,21] Recent studies have demonstrated a rich structural chemistry for these SAMs.[22] The average chain structures (revealed largely by infrared spectroscopy) are now known to reflect much more complex multichain unit cells. Structural characterization of *substituted* *n*-alkanethiolate SAMs on silver has received little attention,[12,13] and only limited data exist for these types of SAMs on gold.[12,13,23-26] The study reported in this paper examines the influences on structure and wetting properties of replacing a $-CH_2-$ group in an internal position of an *n*-alkanethiolate monolayer with an ether oxygen atom (−O−). We have chosen to study the ether group for several reasons. First, it is similar in size and shape to a methylene group. Second, the required compounds are easily synthesized. Third, alkyl ethers demonstrate interesting conformational properties that are unlike those of simple *n*-alkanes.[27] We use two complementary spectroscopic methods—reflection absorption infrared spectroscopy (RAIRS) and sum-frequency generation spectroscopy (SFS)—as well as XPS and ellipsometry to examine the structural consequences of this replacement both in the interior of the film and at the region of the film nearest the monolayer/air interface. We also examine its effect on the interfacial properties of the SAM as deduced from measurements of wetting properties.

In SAMs derived from *n*-alkanethiols on silver and gold, the polymethylene chains extend in a trans-zig−zag fashion, contain few gauche conformers, and differ primarily in the degree to which the chains tilt away from the surface normal.[4,7,8] The different structures adopted by the hydrocarbon chains in the SAMs are related to the different arrangements of the thiolates that form on the two metal surfaces.[28,29] On Au(111), the thiolates form a $(\sqrt{3} \times \sqrt{3})R30°$ adlayer and are separated from each other by 5.0 Å. This structure results in a packing density (21.4 Å²/thiolate) that is larger than the cross-sectional area of the polymethylene chain (18.4 Å²); as a result, the chains tilt by ~30° from the surface normal to achieve van der Waals contact. On Ag(111), the thiolates also adopt a hexagonal structure but achieve a packing density that is approximately equal to the cross section of the adsorbate: for $CH_3(CH_2)_{17}S$, the nearest neighbor distance is 4.7 Å (19.1 Å²/thiolate). As a

† Harvard University.
‡ Massachusetts Institute of Technology.
§ Oxford University.
⊥ University of Illinois at Urbana-Champaign.
⊗ Abstract published in *Advance ACS Abstracts*, May 1, 1995.

0022-3654/95/2099-7663$09.00/0

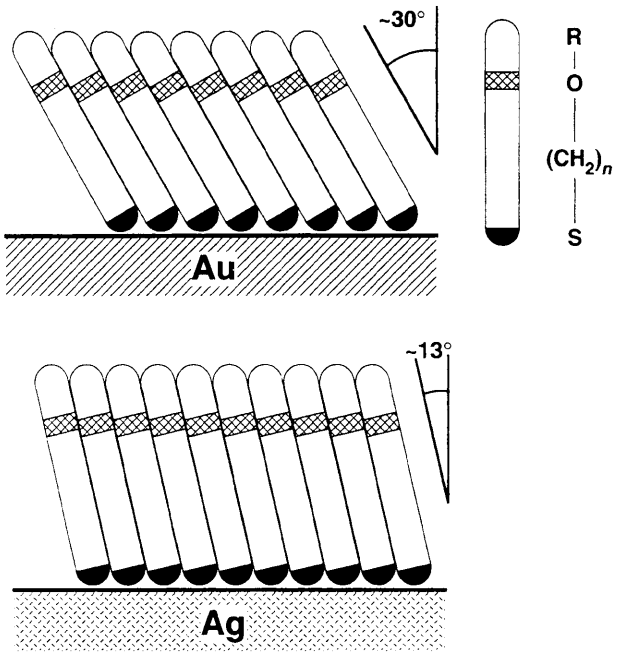

Figure 1. Schematic idealized illustration of ω-alkoxy-*n*-alkanethiolate monolayers formed on gold and silver surfaces. The cants of the axis of the chain have been assumed to be 30° and 13° on gold and silver, respectively, by analogy to monolayers derived from simple *n*-alkanethiols on the two metals.

result, the hydrocarbon chains of *n*-alkanethiolate SAMs on silver cant less from the surface normal ($\lesssim$ 12°) than in SAMs on gold. For the molecules employed in this study, the cross-sectional areas of the ether moieties are approximately the same as that of an unsubstituted polymethylene chain and we might expect that the broad structural features would not be perturbed by the substitution.[30] The schematic structures given in Figure 1 thus would represent the monolayers of ω-alkoxy-*n*-alkanethiolates supported on gold and silver if indeed they are simply isostructural with the corresponding *n*-alkanethiolate overlayers formed on these metals. It is known that the oxygen heteroatom influences the chain conformations and ordering of aliphatic ethers in the solid state in ways that might obviate these latter assumptions.[27] For example, the ether moiety possesses a significant permanent dipole moment, which might be expected to exert a significant electrostatic effect on chain ordering. These functions also promote gauche conformations, generally favoring them over trans by 0.1−0.2 kcal/mol;[27] this fact underlies the conformational "flexibility" typically associated with the ether linkage.

We expect, therefore, that the incorporation of an oxygen heteroatom into the SAM should promote local disordering within the film. For *n*-alkanethiolate SAMs, the highest density of gauche conformers has been suggested, from both experimental[18] and computational studies,[31] to exist at the ends of the chains. The exact placement of the ether is therefore expected to be a critical factor in determining its influence on what is already a conformationally inhomogeneous structure. We expect that placement near the chain ends would affect the structure more significantly than would a substitution in the interior. The magnitude of the effect also should be sensitive to the absolute value of the chain cant, and as a result the phase behaviors on silver and gold should differ to some degree.

In the present study, we use various spectroscopies to examine the conformational disorder present within the monolayers. We rely on sum-frequency and IR spectroscopies to examine the extent to which the presence of the ether oxygen atom disorders a distinct site—a methyl group—that is separated from the heteroatom by one to five methylene units. As the interchain spacings of the SAMs on silver are shorter than those on gold, we exploit this difference to examine the effect of this parameter on the structural and phase behaviors of the SAM.

Wetting, a sensitive measure of the surface free energy of an interface, is also used to characterize these materials. In this study, we have incorporated a polar ether oxygen into a nonpolar hydrocarbon framework. The wetting properties of these SAMs by both polar and nonpolar liquids provide, in a qualitative sense, a measure of the accessibility between the probe liquids and this polar functionality. The probe liquids may influence the structure of the SAMs, and we discuss the comparisons that can be made between the wetting data and the IR and SF spectra that were obtained with SAMs in contact with air.

We note that no crystal structures of long chain alkyl ethers—compounds that are structurally analogous to the SAMs studied here—are available, owing in large part to the difficulty of growing X-ray-quality crystals. Self-assembled monolayers incorporate an ordered anchoring point and thus provide a method for examining some of the features of poorly ordered solid-state structures. We compare the properties of SAMs containing ether groups with related properties of di-*n*-alkyl ethers in the solid state.

Results

Before presenting the results of our studies, we provide an overview of the procedures used to prepare our materials. Recent studies have noted that alkanethiolate SAMs on silver and gold are derived under conditions of kinetic control.[32] The results reported thus reflect the specific protocols described below.

Preparation of SAMs on Gold and Silver. The ω-alkoxy-*n*-alkanethiols were prepared by a straightforward three-step synthesis (eq 1; n = 8, 11, 16); the thiols were purified by column chromatography. Monolayers were prepared by exposing freshly evaporated gold and silver coated silicon wafers[29] to 1 mM deoxygenated ethanolic solutions of the thiols for 18 to 36 h at ~25 °C; silver films were transferred from the evaporator into adsorption solutions under a blanket of argon to minimize their exposure to atmospheric dioxygen. No changes were detected by wetting, ellipsometry, or XPS for SAMs prepared on gold after weeks of exposure to the contacting solution. For silver, slight variations in the wetting and XPS data were detected after days of exposure to the contacting solution (ones we believe are due to surface roughening). We have observed that the extended exposure of silver to alkanethiols forms a layer of Ag_2S between the silver and the adsorbed thiolate.[8] For this reason, the data we present are for SAMs for which the silver substrate was exposed to the alkanethiol for less than 2 days. We focus most of our attention on the properties of SAMs derived from $HS(CH_2)_{16}OR$ (R = methyl to hexyl) because this chain length (C_{16}) yields unsubstituted SAMs of quality superior to that of SAMs containing fewer methylene units. Limited data on SAMs derived from $HS(CH_2)_nOR$ (n = 8, R = methyl and n = 11, R = methyl to propyl) were also obtained on gold and silver; these data are included in the figures whenever possible.

$$H_2C{=}CH(CH_2)_{n-2}Br \xrightarrow[2.\ CH_3COSH/h\nu]{1.\ NaOR/ROH} HS(CH_2)_nOR \quad (1)$$
$$3.\ NaOCH_3/CH_3OH$$

Ellipsometric Thickness of SAMs on Gold. Figure 2 displays the thicknesses of monolayers on gold derived from exposure to ~1 mM ethanolic solutions of various ω-alkoxy-alkanethiols. The data are fit by a line that has a slope of ~1.4

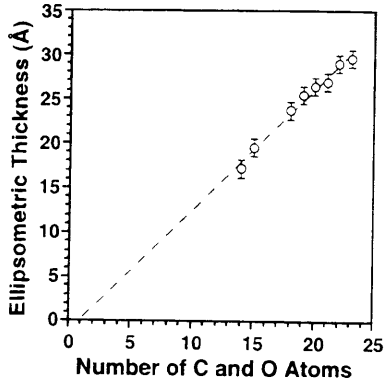

Figure 2. Ellipsometric thicknesses of monolayers formed by exposure of gold surfaces to ~1 mM ethanolic solutions of $HS(CH_2)_nOR$ for 18–36 h. The x-axis is linear in the total number of carbon and oxygen atoms in the adsorbate. The dashed line is a least squares fit to the data: $y(Å) = 1.4x - 1.2$.

Å/CH_2 and a negative intercept. This slope is consistent with the value of 1.5 Å/CH_2 obtained for n-alkanethiolate SAMs on gold by others.[4,7] This similarity suggests that the ether oxygen atom does not dramatically disorder the SAM and the SAMs derived from the ω-alkoxyalkanethiols have a similar canted-chain structure. We interpret the negative intercept (Figure 2) to indicate the displacement of adventitious materials from the surface of the gold upon adsorption of the thiols.[5]

We did not conduct analogous ellipsometric studies on the SAMs that form on silver, as these measurements could not be performed without exposing the unfunctionalized silver to the atmosphere.[8] We have previously observed that high quality SAMs are obtained more reproducibly when the bare silver surfaces are minimally exposed to the atmosphere.[8,9]

X-ray Photoelectron Spectroscopy (XPS). We also used XPS to measure the thicknesses of the SAMs. This measurement relies on the attenuation of the photoelectron signal from the underlying metal by the SAM (eq 2) and provides a method for comparing the *relative* thicknesses of the SAMs.[8,9,33] In eq

$$\ln I(n) = \frac{-nd\cos\alpha}{\lambda\cos\phi} + \ln(\beta I_0) \qquad (2)$$

2, $I(n)$ is the attenuated intensity of photoelectrons from the substrate, n is the number of carbon atoms in the adsorbate, d is the incremental contribution of a methylene unit to the length of a trans-zig–zag n-alkyl chain (=1.27 Å/CH_2),[34] α is the angle that the axis of the hydrocarbon chain is canted relative to the surface normal, λ is the escape depth of photoelectrons from the substrate through hydrocarbon (Å), ϕ is the angle the detector is oriented relative to the surface normal (=55°), β represents the attenuation due to the thiolate and ether oxygen atom, and I_0 is the intensity of photoelectrons from a clean substrate. We previously have used this method to characterize the mass coverage (i.e., thickness) of n-alkanethiolate SAMs on gold and silver.[8,9,33] This method has a decided advantage for SAMs on silver over ellipsometry in that no measurements are required on the underivatized substrates.

Parts a and b of Figure 3 display the intensities of the Au(4f) and Ag(3d) photoelectrons for ω-alkoxy-n-alkanethiolate SAMs on the two metals. The slopes of the lines in these figures are within 10% of those observed for unsubstituted SAMs on these metals,[35] with the value on gold approximating that expected for a hydrocarbon chain that is canted ~30° from the surface normal and the value on silver being close to that for a chain oriented along the surface normal direction. These observations are consistent with the schematic illustrations given in Figure 1.

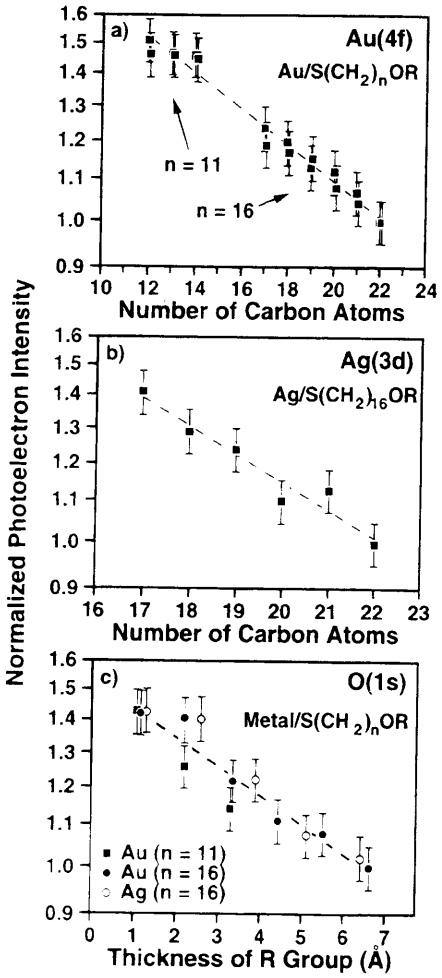

Figure 3. Intensities of photoelectrons from the underlying substrates and the ether oxygen for SAMs derived from $HS(CH_2)_nOR$ on gold and silver. Dashed lines represent least squares fits to the data as presented (eq 2). Data represent single measurements and have an error of ~5%. In a and b, the x-axis is linear in the total number of carbon atoms in the adsorbate. The data were normalized to the photoelectron intensities obtained for a SAM derived from $HS(CH_2)_{16}O(CH_2)_5CH_3$. The slopes of the dashed lines (Au(4f), −0.041; Ag(3d), −0.064) are comparable to results using unsubstituted n-alkanethiols (Au(4f), −0.046; Ag(3d), −0.060). In c, the thicknesses of the R groups on the two metals were estimated by assuming the canted structures of Figure 1. The slope of the dashed line for the O(1s) photoelectrons (kinetic energy = 953 eV) is −0.067/Å and is comparable to the slope of −0.061/Å for Au($4p_{3/2}$) photoelectrons (kinetic energy = 940 eV) through n-alkanethiolate SAMs on gold.[35]

We also examined the attenuation of O(1s) photoelectrons for the ether oxygen atoms of the SAMs as the R group was varied. Because of its low concentration (i.e., a monolayer) and the lower sensitivity of XPS to oxygen than to gold or silver, Figure 3c combines data from SAMs on silver and gold. We have plotted these data together by weighting the number of carbon units in the R group by the contribution that a CH_2 unit makes to the thickness of an n-alkanethiolate SAM on these metals (Figure 1: ~1.10 Å/CH_2 and ~1.27 Å/CH_2 on Au and Ag, respectively). In Figure 3c, the rate of attenuation of the O(1s) photoelectrons by the R groups is comparable (within 10%) to that of photoelectrons of similar kinetic energy—Au($4p_{3/2}$) photoelectrons—by n-alkanethiolate layers.[35] This observation suggests that the structure of the R group in these SAMs, as detected by XPS, is similar to the structure of n-alkanethiolate SAMs on the respective metals. We must emphasize, however, that this analysis is at best a grossly qualitative one given the limited range of the data (i.e., the mean free paths at these

TABLE 1: Wetting Data, O(1s) Photoelectron Binding Energies, and Ellipsometric Thicknesses (d) for SAMs of $HS(CH_2)_nOR$ Adsorbed on Gold Surfaces

		contact angles[a] (advancing, receding; deg)								
n	R	water	Gly	Form	EG	BN	BCH	HD	O(1s)[b] (eV)	d[c] (Å)
8	methyl	82, 69	75, 61	68, 56	37, –	29, –	<15, –	<15, –		10
11	H	<15, –	<15, –	<15, –	<15, –	<15, –	<15, –	<15, –		
11	methyl	85, 72	83, 69	78, 65	60, 44	59, 40	47, 30	37, 11	532.92	
11	ethyl	96, 86	94, 83	85, 78	68, 60	66, 47	52, 38	43, 28	532.69	17
11	propyl	104, 95	96, 85	91, 85	73, 63	69, 51	52, 39	44, 31	532.62	19.5
16	H	<15, –	<15, –	<15, –	<15, –	<15, –	<15, –	<15, –	532.92	
16	methyl	85, 73	87, 74	80, 69	62, 51	64, 43	52, 39	44, 29	533.01[d]	24
16	ethyl	99, 88	96, 85	92, 83	74, 65	71, 54	58, 45	49, 35	532.74[d]	25.5
16	propyl	110, 99	98, 88	96, 87	76, 66	71, 56	56, 45	48, 35	532.68[d]	26.5
16	butyl	113, 101	100, 89	97, 89	77, 68	73, 55	57, 45	48, 34	532.63	27
16	pentyl	115, 101		96, 91	78, 71	73, 58	58, 46	48, 33	532.62	29
16	hexyl	115, 103	101, 89	95, 89	78, 70	73, 59	57, 46	48, 35	532.61[d]	30
octadecanethiol		116, 105	102, 90	97, 90	78, 69	74, 56	59, 46	48, 34	NA	

[a] Gly = glycerol, Form = formamide, EG = ethylene glycol, BN = α-bromonaphthalene, BCH = bicyclohexyl, HD = hexadecane. Values are ±2°. Receding contact angles where the contacting liquid continued to wet the surfaces upon removal are signified with a dash. [b] O(1s) photoelectron binding energies measured relative to $Au(4f_{7/2}) = 84.00$ eV. Values are ±0.02 eV. NA = not applicable. [c] Ellipsometric thicknesses were estimated using a refractive index of 1.45. Values are ±2 Å. [d] The O(1s) binding energies (±0.05 eV) of polycrystalline samples of n-$C_{22}H_{45}OR$ were measured to be as follows: R = methyl, 532.84 eV; ethyl, 532.71 eV; propyl, 532.71 eV; hexyl, 532.58 eV. Values were referenced by setting the C(1s) binding energy of the polymethylene peak to the average value (284.91 eV) obtained using the SAMs on gold.

TABLE 2: Wetting Data and O(1s) Photoelectron Binding Energies for SAMs of $HS(CH_2)_nOR$ Adsorbed on Silver Surfaces

		contact angles[a] (advancing, receding; deg)							
n	R	water	Gly	Form	EG	BN	BCH	HD	O(1s)[b] (eV)
8	methyl	82, 63	80, 61	72, 61	53, 37	56, 28	41, 14	33, –	
11	H	<15, –	<15, –	<15, –	<15, –	<15, –	<15, –	<15, –	
11	methyl	84, 66	83, 64	75, 62	56, 40	60, 34	46, 27	38, 20	
11	ethyl	99, 82	94, 84	90, 78	66, 52	66, 39	49, 28	43, 27	
11	propyl	109, 93	100, 83	93, 83	73, 62	69, 40	52, 33	46, 31	
16	H	<15, –	<15, –	<15, –	<15, –	<15, –	<15, –	<15, –	
16	methyl	86, 75	86, 75	81, 70	65, 55	65, 39	53, 38	47, 31	532.90
16	ethyl	103, 92	99, 84	93, 86	74, 66	73, 44	58, 40	49, 33	532.64
16	propyl	115, 102	100, 84	97, 85	74, 63	72, 43	57, 42	48, 33	532.66
16	butyl	117, 101	102, 89	98, 89	77, 68	74, 45	57, 37	50, 30	532.64
16	pentyl	118, 99	101, 91	99, 90	77, 69	73, 45	57, 38	50, 33	532.61
16	hexyl	116, 99	100, 93	98, 90	77, 66	74, 44	57, 39	48, 31	
octadecanethiol		116, 104	103, 91	100, 89	77, 66	73, 46	57, 38	49, 33	NA

[a] Abbreviations are the same as in Table 1*a*. Values are ±2°. [b] O(1s) photoelectron binding energies (±0.05 eV) measured relative to $Ag(3d_{5/2}) = 367.85$ eV. NA = not applicable.

energies are large compared to the incremental thickness added per carbon atom).

We also obtained high resolution XP spectra of the C(1s) and O(1s) spectral regions for the SAMs and observed differences (of ~0.4 eV) in the binding energies of the O(1s) peak and the C(1s) peaks for carbon atoms adjacent to the oxygen atom as the length of the R group was varied (Tables 1 and 2 and supplementary materials). We found that the methyl ether exhibited O(1s) and C(1s) peaks at higher binding energies than are seen in the spectra of the other ethers; the O(1s) and C(1s) peak positions in the XP spectra for the butyl, pentyl, and hexyl ethers were the same and defined the other limit of this binding energy shift. A similar trend was observed in the XP spectra of solid-state samples (polycrystalline n-docosyl alkyl ethers—see supplementary materials). We interpret these differences as being due primarily to final state effects reflecting the different screenings of the photogenerated core hole by the local environment.

Reflection Absorption Infrared Spectroscopy (RAIRS). Infrared spectroscopy has been an invaluable technique for characterizing SAMs.[4,7,8,18,23–26] A particular strength of this technique is its ability to characterize both the average orientation of the hydrocarbon chains and the degree of conformational disorder present within the SAM. The interpretations of the RAIRS data presented below rely on the interpretations and methods developed in earlier studies of n-alkanethiolate SAMs on silver and gold.[4,9,18,20] These have been discussed in detail elsewhere and will not be repeated here.

Figure 4 shows infrared spectra in the C–H stretching region of SAMs derived from $HS(CH_2)_nOCH_3$ (n = 8, 11, and 16) on silver and gold substrates. Figure 5 presents data for a homologous series of SAMs on silver and gold using thiols of the general structure $HS(CH_2)_{16}OR$, where R = methyl to hexyl units. The data and relevant mode assignments, where known, are summarized in Tables 3 and 4.[4,12,18,36–38] Several systematic trends are evidenced in these data, particularly when compared with the spectra for unsubstituted n-alkanethiolate SAMs on silver and gold (Figure 6). We consider the spectral data for the methyl ethers on silver and gold first.

(1) Methyl Ethers. The spectra of the methyl ether SAMs in the C–H stretching region are complex and not completely understood. The relevant mode assignments have been discussed elsewhere[12] and will be only summarized here. In the spectrum for n = 16, the assignment of the modes for the methylene stretching vibrations is straightforward. The antisymmetric C–H stretching modes (d^-) appear at 2919 cm^{-1} on Au and 2920 cm^{-1} on Ag; the symmetric (d^+) modes appear at 2851 and at 2850 cm^{-1}, respectively. Assignment of these bands in any of the other spectra is difficult owing, at least in part, to the overlap of other bands occurring in these regions. The bands at 2810, 2830, and 2982 cm^{-1} are all due to C–H stretching fundamentals of the methyl group. The presence of

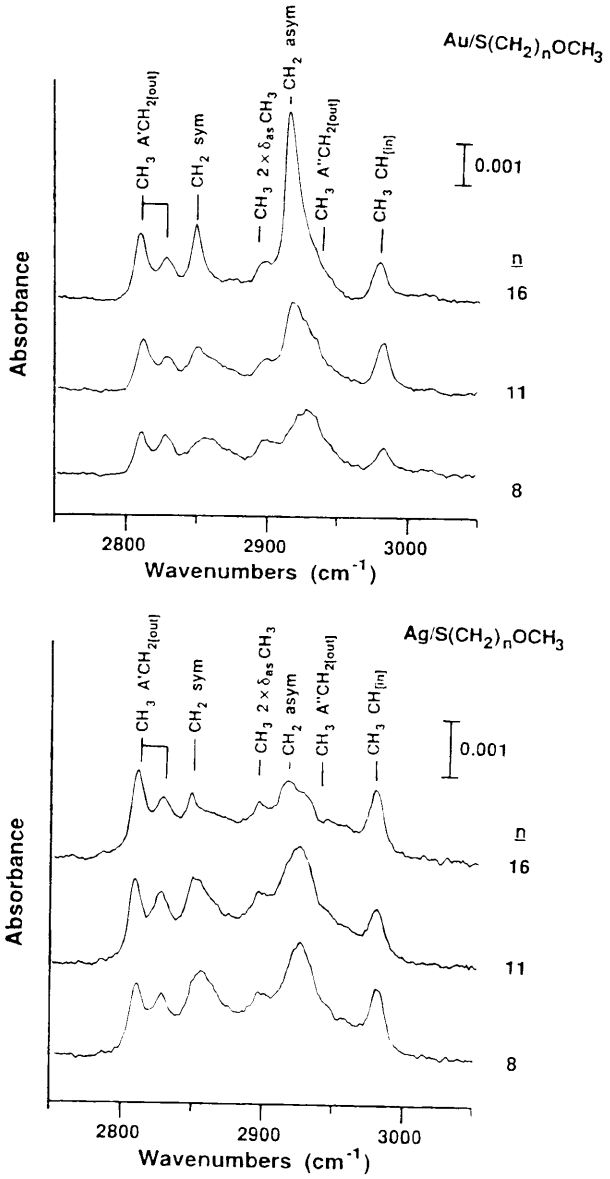

Figure 4. RAIRS of monolayers of $HS(CH_2)_nOCH_3$ (n = 8, 11, and 16) adsorbed on gold (upper panel) and silver (lower panel) from ethanol. The spectra have been offset vertically for clarity.

two bands at lower frequency is believed to reflect splitting due to Fermi resonance. The broad band centered at ~2900 cm^{-1} is assigned to an overtone of the antisymmetric method bending mode.

It is most striking that, for n = 8 and 11, the spectra on both silver and gold exhibit other features in the vicinity of the d^+ and d^- modes. In all the spectra, the line shapes of these latter bands are highly asymmetric, exhibiting pronounced tails at high frequency. We believe that some of the structure seen in the region of the d^- band is due to the contribution of an additional unresolved out-of-plane C−H stretching mode of the methyl group and that other perturbations are also present. For example, the oxygen heteroatom is expected to perturb the frequencies (and perhaps the intensities) of the C−H stretching modes of the neighboring methylene groups; such interactions are expected to shift these modes to higher frequency. We also believe that the chains in the SAMs may contain a fair degree of conformational disorder near the chain ends. Such conformations would weight the spectra on the high frequency side of the d^+ and d^- bands. Still, the data suggest (see below) that the predominant conformation of the chain is trans-zig−zag, as has been documented for the unsubstituted n-alkanethiolate SAMs on these same metals.[4,8,9]

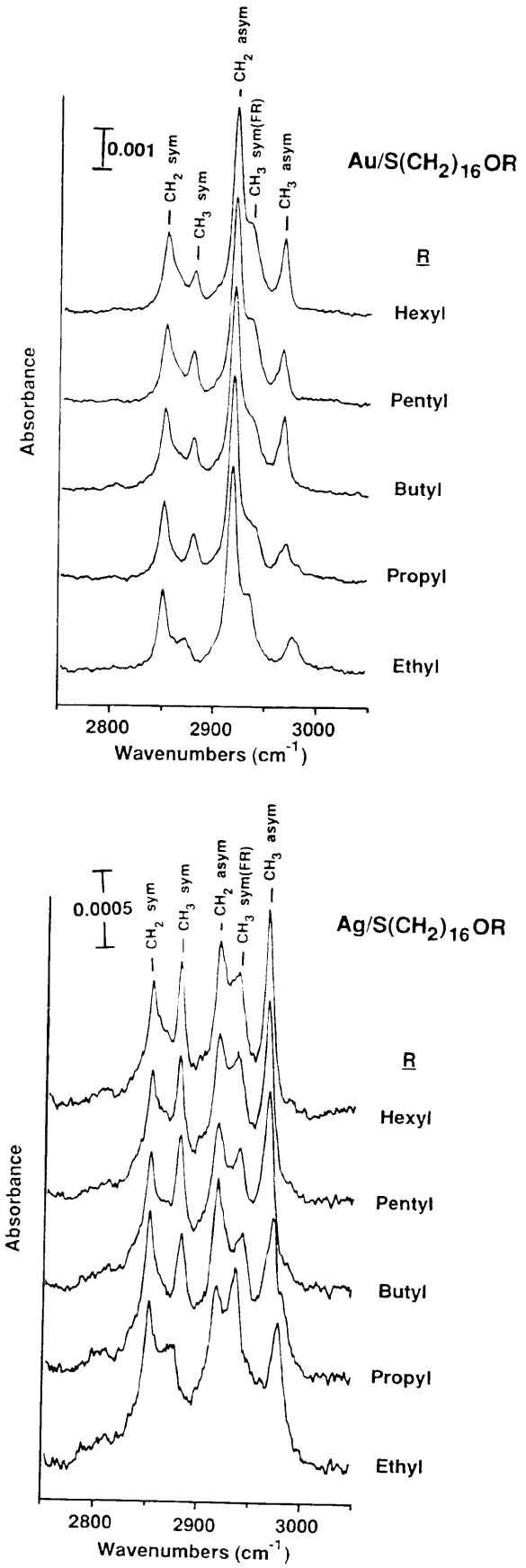

Figure 5. RAIRS of monolayers of $HS(CH_2)_{16}OR$ adsorbed on gold (upper panel) and silver (lower panel). C−H stretching mode abbreviations: asym = asymmetric, sym = symmetric, FR = Fermi resonance. The spectra have been offset vertically for clarity.

Inspection of the methyl C−H stretching modes reveals an interesting perturbation due to chain length. For SAMs on both silver and gold, the intensity patterns of the various methyl

TABLE 3: IR Peak Assignments for Monolayers of $HS(CH_2)_nOCH_3$ on Gold and Silver (cm^{-1})

	Au			Ag		
mode description[a]	$n = 8$	$n = 11$	$n = 16$	$n = 8$	$n = 11$	$n = 16$
CH_3, A′ $CH_{2\text{out}}$	2811	2812	2810	2812	2811	2811
	2829	2830	2829	2830	2830	2830
CH_2, sym (d^-)	2858[b]	2852	2851	2857[b]	2853[b]	2850
CH_3, $2 \times \delta_{as}$ CH_3	2900	2900	2899	2901	2900	2899
CH_2, asym (d^-)	2926[b]	2920[b]	2919	2926[b]	2923[b]	2920[b]
CH_3, A″ $CH_{2\text{out}}$	c	c	c	c	c	c
CH_3, CH_{in}	2984	2983	2982	2982	2982	2982

[a] Assignments of peaks from refs 4, 18, 36, and 37. [b] Multiple unresolved components. [c] Unresolved shoulder.

modes are hard to understand if a single conformational profile of the chain were conserved for all values of n. We find, for example, that the spectra of the methyl modes for both odd and even values of n are similar; indeed, the SAMs on silver and on gold do not differ significantly. This latter observation is remarkable, given the significant differences in the chain cant angles for the polymethylene chains on these two metals. The data thus seem to suggest that a significant degree of reconstruction characterizes the methyl surface in the methoxy-terminated SAMs.

The spectral intensities of the d^+ and d^- modes are, as expected, consistent with the presence of specifically canted chains; on silver the inclinations are small (<12°), while on gold they are larger (>24°). The data therefore suggest that the methyl ether SAMs have molecular architectures that are, for the most part, similar to those of the n-alkanethiolates, with the exception that the methyl surface relaxes considerably from the projections (i.e., orientations) expected on the basis of the organization of the polymethylene chain. The specific organization of the chains on silver and gold is discussed in more quantitative terms below.

(2) Ethyl to Hexyl Ethers. The data presented in Figure 5 demonstrate that the organization of the chain and the perturbation of that structure caused by the O atom are highly sensitive to the substitution pattern of the ether. The SAMs examined here are ones in which the absolute position of the oxygen atom is held fixed from the metal surface by a tether containing 16 methylene units, while an additional linear hydrocarbon chain of up to 6 carbons is appended to the top. The data show a smooth progression of the SAM to a structure that is completely analogous to that of unsubstituted n-alkanethiolate SAMs (when the length of the alkoxy group is increased to a butyl group or longer). Most telling in this regard is the intensity patterns associated with the methyl groups; the relevant mode assignments are summarized in Table 4.

The r_a^- and r^+ modes for SAMs (R = butyl to hexyl units) on both silver and gold show the same absolute and relative intensities as are seen in corresponding SAMs of n-alkanethiolates. The pronounced modulation of the band intensities seen in SAMs on gold (Figures 5a and 6a) is especially striking. These data compel the conclusion that the surface densities and molecular orientations of methyl groups in these SAMs are similar to those found in the simpler unsubstituted n-alkane-based SAMs. The structure we infer is thus one based on canted chains whose organization is relatively unperturbed by the O heteroatom. This notion is also confirmed by an independent analysis of the modes associated with the methylene groups. The picture that emerges is that the addition of even a relatively short chain—here of the order of a butyl group—is sufficient for removing the conformational perturbations due to the ether oxygen; the chain adopts a predominantly trans-zig−zag geometry, and the oxygen serves, then, as an innocent replacement for a methylene group.

The SAMs on gold and silver are quite different in how the chain length influences the spectra. The data for the SAMs on gold clearly reveal that the absolute length of the chain—that is, whether the chain contains an odd or even number of methylene units—fixes the organization of the methyl surface. This odd−even behavior in the structure of the terminal methyl group probably reflects the adoption of a fixed value and sign of the bond angle that characterizes the Au−S bonding. The SAM on gold adopts a positive value of the angle of inclination (the tilt angle α as it is defined in Figure 7), and this value is conserved for all chain lengths. The SAMs on silver are apparently different, as the structure of the methyl surface is insensitive to chain length for all ethers that are equal to or longer than a butyl unit. This behavior follows exactly the pattern seen in the n-alkanethiolate SAMs on silver (Figure 6b).[8,9] We have interpreted this behavior in the past as being an indication that surface tension minimization may act in this system to choose the absolute direction of the chain cant.[9]

For ethers shorter than R = butyl, the spectra observed are complex. We believe that some of the complexities reflect the intrinsic perturbations expected for groups interacting with the oxygen atom, although perturbation of the conformational state of the chain also appears to be important here as well. We are uncertain as to the importance of the role played by each, so the finer details of these intermediate structures cannot be established unambiguously. We note, however, that the role of electronic perturbations is quite significant. The SAMs on silver, for example, have relatively minor chain cants (α < 12°), while those on gold are much larger (α > 25°). The density of any gauche conformations is expected, as a result, to be higher on gold given that the nearest neighbor spacing is fixed in the SAMs. In the spectra of both SAMs, however, we see the same qualitative trends exhibited in the spectra. The methyl modes are "perturbed" in comparable ways in both the ethyl and propyl systems on both silver and gold.

We finally turn to a consideration of the CH_2 stretching vibrations. Both the d^+ and d^- modes exhibit significant shoulders at higher frequency. The structure of the bands is not one that might be assumed simply to be a reflection of a single homogeneous population of methylenes. The key, then, is to establish the factors that contribute the most (the presence of multiple conformations, intrinsic perturbations of force constants due to the presence of the heteroatom, etc.). The resolution of this point influences strongly the certainty with which the average chain tilt angle, α, can be calculated. For the current discussion, we invoke only qualitative analyses of the spectra and forgo the more detailed simulations we have reported in the past[9,23] since the latter are not needed to address the present issue.

It is well-known that an oxygen heteroatom significantly perturbs the vibrational frequencies of a methylene group.[38] We have seen these effects before in SAMs of hydroxyl-terminated thiols of the structure $HS(CH_2)_{16}OH$.[23] We therefore expect the methylenes adjacent to the ether oxygen moiety to show distinct features in the C−H stretching region. The d^- mode is an instructive one to consider. Some of the intensity of the shoulder at ~2930 cm^{-1} is due to the r^+ (Fermi resonance) component of the methyl group, although all of it cannot be of this origin. The remainder is thus likely due to some other component; conformations and the perturbations due to the heteroatom appear to be the most likely candidates. The frequency shift associated with "chain melting" is generally much larger for the d^- than for the d^+ mode. In the present spectra, the asymmetries are of comparable magnitude and relative intensity in each. Their weighted contribution is also weakly perturbed by increasing the chain length of the terminal

TABLE 4: IR Peak Assignments for Monolayers of $HS(CH_2)_{16}OR$ on Gold and Silver (cm^{-1})

	Au						Ag					
mode description[a]	R = Et	R = Pr	R = Bu	R = Pe	R = Hx	ODT[b]	R = Et	R = Pr	R = Bu	R = Pe	R = Hx	ODT[b]
CH_2, sym (d^+)	2850	2850	2851	2850	2851	2850	2851	2851	2851	2851	2851	2850
CH_3, sym (r^+)	2872	2881	2879	2878	2878	2878	~2873[c]	2882	2880	2879	2879	2878
CH_2, asym (d^-)	2919	2918	2918	2918	2918	2917	2919	2918	2917	2917	2918	2918
CH_3, sym (r^+,FR)[d]	~2938	~2939	2936	2934	2933	2938	2937	2940	2938	2936	2935	2935
CH_3, asym (r_a^-)[e]	~2978[c]	~2971[c]	2967	2966	2966	2965	~2978	2972	2967	2966	2965	2964

[a] Assignments of peaks from refs 4, 18, and 36. [b] ODT = n-octadecanethiol. Data from refs 4 (Au) and 7 (Ag). [c] Multiple unresolved components. [d] FR = Fermi resonance splitting component, unresolved shoulder. [e] The frequencies of the out-of-plane mode (r_b^-) are uncertain given the weak appearance of this band as an unresolved shoulder on the lower frequency side of the r_a^- mode.

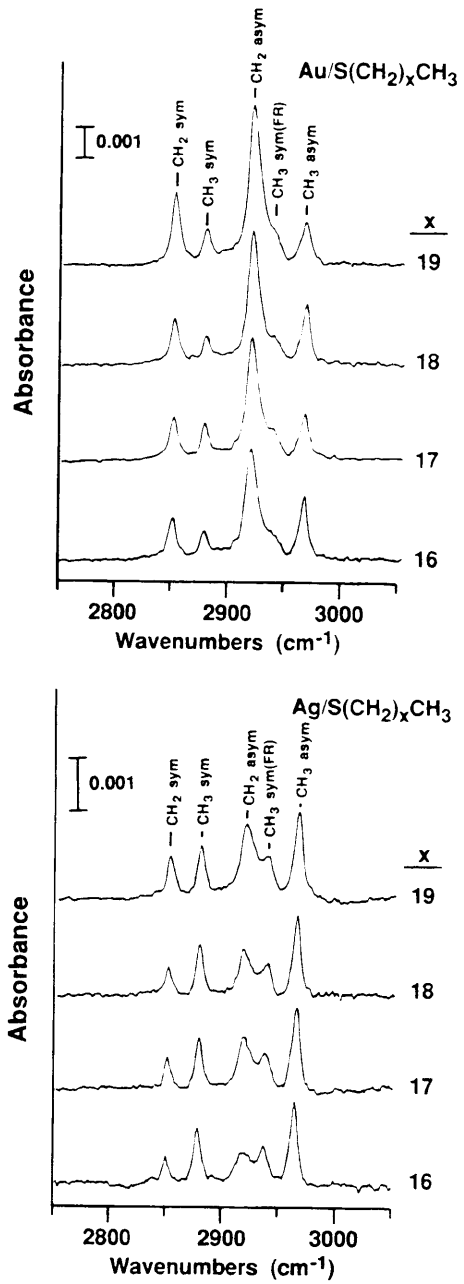

Figure 6. RAIRS of monolayers of unsubstituted n-alkanethiols $HS(CH_2)_xCH_3$ adsorbed on gold (upper panel) and silver (lower panel). C−H stretching mode abbreviations: asym = asymmetric, sym = symmetric, FR = Fermi resonance. The spectra have been offset vertically for clarity.

alkoxy group from butyl through hexyl.[8] We thus conclude that the bulk of the band asymmetry seen in the d^+ and d^- modes is due to the intrinsic perturbations of the methylenes by the heteroatom. The data can therefore be interpreted as being consistent with a simple all-trans canted structure of the chains,

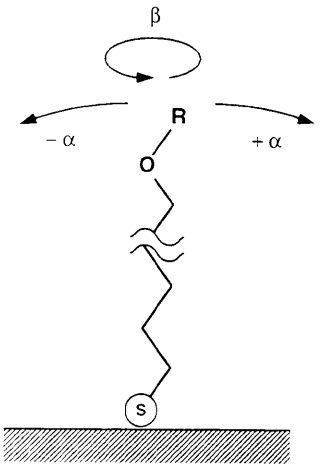

Figure 7. Schematic diagram of an all-trans chain in an n-alkanethiolate monolayer on a surface. The illustration defines the sign conventions and reference values for the cant angle (α) and the chain twist (β).

where (according to the scheme above) $\alpha \cong 26°$ and $\beta \cong 52°$ on gold and $|\alpha| \cong 12°$ and $\beta \cong 45°$ on silver when R = butyl, pentyl, and hexyl.

Two further experiments were conducted to confirm these interpretations. The first involved the synthesis of specifically deuterated isotopomers of the SAMs. These materials allow a crude separation of the spectral contributions which originate in the functions present on either side ofthe oxygen atom. These spectra (included in the supplementary materials) are not completely unambiguous in their interpretation since it is clear that coupling occurs across the "dividing line" and that the spectra of either half cannot be completely separated in this way. Even so, the following general conclusion was reached. The portion of the chain below the O atom is best described by a largely all-trans chain whose organization and orientation is analogous to the parent n-alkanethiolate SAMs. The conformations of the region above the oxygen atom—for example, the conformation of the terminal outer alkoxy group—are less clearly distinguished.

A more powerful demonstration of the equilibrium organization of the chain came from an analysis of the dependence of the spectra on surface temperature. Figure 8 shows data for a hexyl ether SAM on gold at several different temperatures between 300 and 78 K. Data are shown for both the C−H stretching region and the lower frequency region between 1000 and 1500 cm^{-1}. The latter allows the examination of various C−H bending modes as well as the fundamentals associated with C−O stretching motions.

At 78 K, the population of gauche conformations in the polymethylene chain is quenched. This spectrum is most consistent with an all-trans structure; the orientation of the methyl is indistinguishable in every way with an isostructural odd-chain-length n-alkanethiolate SAM on gold. For example, we see a clear definition of both the in-plane and out-of-plane antisymmetric stretches in these data (r_a^- and r_b^-) at 2965 and

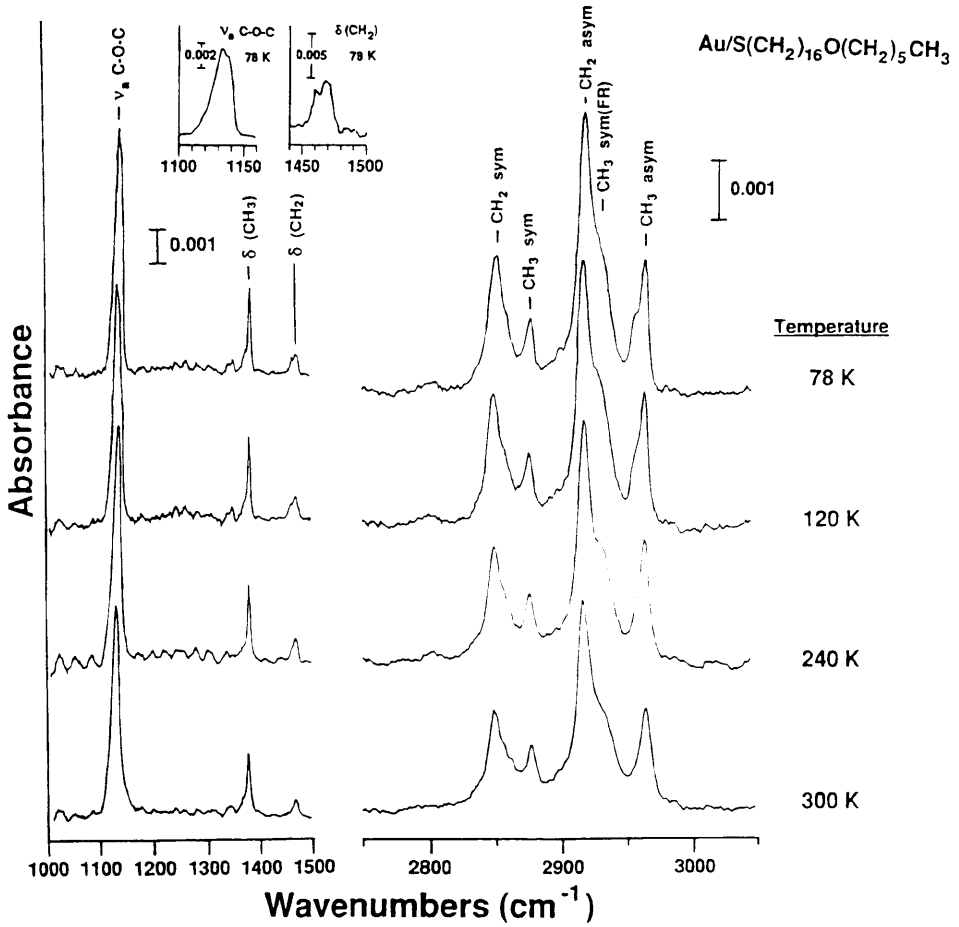

Figure 8. Effect of temperature on the IR spectrum of $HS(CH_2)_{16}O(CH_2)_5CH_3$ adsorbed on gold. The stretching mode abbreviations are the same as in Figure 5 with δ denoting a scissor deformation. The spectra have been offset vertically for clarity. The insets contain expanded spectra of the ν_a(C−O−C) and $\delta(CH_2)$ modes at 78 K.

2957 cm^{-1}, respectively, which exactly follows that seen in the latter SAMs. Note, also, that the band asymmetries seen on the d^- and d^+ bands sharpen and become more clearly defined. An additional, and as yet not understood, band grows in at 2899 cm^{-1}. We further find that many of the bands in the low frequency region compel the assignment of an all-trans structure. The band at ~1135 cm^{-1}, assignable to the antisymmetric C−O−C stretching motion of a trans-conformer, is perhaps the most instructive feature in this regard. Multiple band splittings also are seen at 78 K; this observation suggests the organization involves, at least in the case of the SAM on gold, a multichain unit cell. We note, for example, that cooling induces a splitting of the C−O−C mode into two poorly resolved components at 1132 and 1137 cm^{-1} (see inset to Figure 8). At 78 K, the CH_2 scissor deformation mode also shows a diagnostic splitting into components at 1460 and 1469 cm^{-1}. Taken together, we see no other possible interpretation other than the minimum energy structure being an all-trans chain with few gauche defects.

The RAIRS data thus reveal that an ether oxygen atom does perturb the organization of the hydrocarbon chain in the SAMs on silver and gold. This perturbation is a relatively weak one. Significant reconstruction of the surface occurs in the methyl ether-containing SAMs on both silver and gold. Appending even a fairly small chain (i.e., a butyl group or larger) is sufficient to outweight the influence of the oxygen atom, and the chain adopts a more typical, nearly all-trans structure. We defer further comment on these points to later in the paper.

Sum-Frequency Spectroscopy (SFS). We have analyzed the monolayers derived from 16-alkoxy-*n*-hexadecanethiols on silver and gold by infrared−visible sum-frequency spectroscopy (SFS). Sum-frequency spectroscopy has been reviewed recently by Eisenthal,[39] and we provide a brief description of the technique here; more details may be found elsewhere.[12,40] SFS is a nonlinear optical technique in which a fixed-frequency, pulsed visible laser and a tunable, pulsed infrared laser are superimposed at an interface and photons emitted at the sum of the two input frequencies are detected.[41] The intensity of the sum-frequency signal depends on the second-order, nonlinear susceptibility of the surface:

$$I_{sum} \propto |\chi^{(2)}_{NR} + \chi^{(2)}_{R}|^2 \quad (3)$$

where $\chi^{(2)}_{NR}$ is the nonresonant susceptibility of the metal substrate, and $\chi^{(2)}_{R}$ is the resonant susceptibility of the adsorbed molecules. $\chi^{(2)}_{NR}$ varies little with infrared frequency and gives rise to a constant background signal in sum-frequency spectra. $\chi^{(2)}_{R}$ is proportional to the product of the IR and Raman transition moments, is averaged over the molecular orientations in the monolayer, and is maximized when the infrared laser is in resonance with a vibrational mode that is both infrared and Raman active. Scanning the frequency of the infrared laser thus yields a vibrational spectrum of molecules at the surface. Since both $\chi^{(2)}_{R}$ and $\chi^{(2)}_{NR}$ are complex quantities, the shapes of peaks in sum-frequency spectra depend on the relative phases of the two susceptibilities.[12,40] The different phases of $\chi^{(2)}_{NR}$ account for the different peak shapes observed in the SF spectra of monolayers on silver and gold.

Figure 9 shows sum-frequency spectra in the C−H stretching region of an archetypical self-assembled monolayer, octadecanethiol on gold and on silver. The visible and infrared lasers and the emitted sum-frequency light were all p-polarized. Both spectra are dominated by three peaks, all arising from the

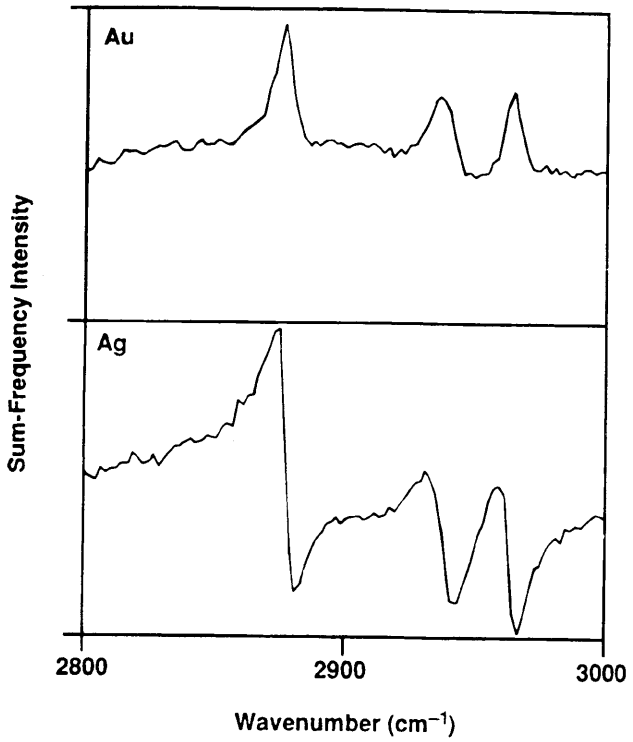

Figure 9. Sum-frequency spectra of monolayers of *n*-octadecanethiol on gold (upper panel) and silver (lower panel). The azimuth represents the wavenumber of the infrared laser. All electric fields at the surface were p-polarized. The nonresonant background arising from the metal–monolayer interface has not been subtrated in these figures. The spectra have been offset vertically for clarity. The peak assignments are the same as in Table 4: r^+, 2878 cm^{-1}; r^+, FR, 2939 cm^{-1}; r_a^-, 2966 cm^{-1}.

terminal methyl group: the symmetric stretch r^+ at 2877 and 2936 cm^{-1} and the in-plane asymmetric stretch r_a^- at 2965 cm^{-1}.[12,40,42] The methylene modes are barely discernable as weak, broad peaks near 2850 and 2900 cm^{-1}. Figure 10 shows SF spectra of $HS(CH_2)_{16}OR$ (R = ethyl to hexyl units) adsorbed on silver and gold, also with all electric fields p-polarized. In the longer ethers (butyl, pentyl, and hexyl), the methyl stretching modes appear at the same frequencies as in the octadecanethiolate SAMs. In the propyl and ethyl ethers, the same three methyl modes are observed, but the frequencies and intensities are perturbed by the proximity of the oxygen atom of the ether.

The first point to note is the similarity between the spectra of the longer chain ethers and the spectrum of octadecanethiol on both silver and gold. The second is the pronounced odd-even intensity variation in the r_a^- mode in the monolayers on gold. This odd–even variation in also present in the simple *n*-alkanethiols on gold:[9,23] however, no such variation occurs on silver.[8,9] The third point is that the methylene modes in the spectra of the ethers adsorbed on silver, though still weak, are more pronounced than in adsorbed octadecanethiol. The influence of the methylene groups is seen most clearly between 2900 and 2920 cm^{-1} in the spectra on silver. On gold, the signal-to-noise in the spectra obtained is not sufficiently good to draw any definitive conclusions about the effect that the incorporation of the ether oxygen atom has on the methylene modes.

The most important finding that emerges from the SFS data relates to the relatively weak features seen for the methylene modes of SAMs on both silver and gold. These weak bands are most consistent with a largely all-trans arrangement of the chains on each metal; the little intensity we do see is likely due to a small population of gauche conformers, although the broken symmetry of the chain ends could contribute here as well. The data show that a small difference exists in the ether layers in this regard as compared to *n*-octadecanethiolate SAMs on silver and gold; however, the data are not sufficient to quantify this difference more rigorously. It is clear though that while low in absolute terms, the larger density of gauche conformations is found in the SAMs that contain the ether unit on both silver and gold.

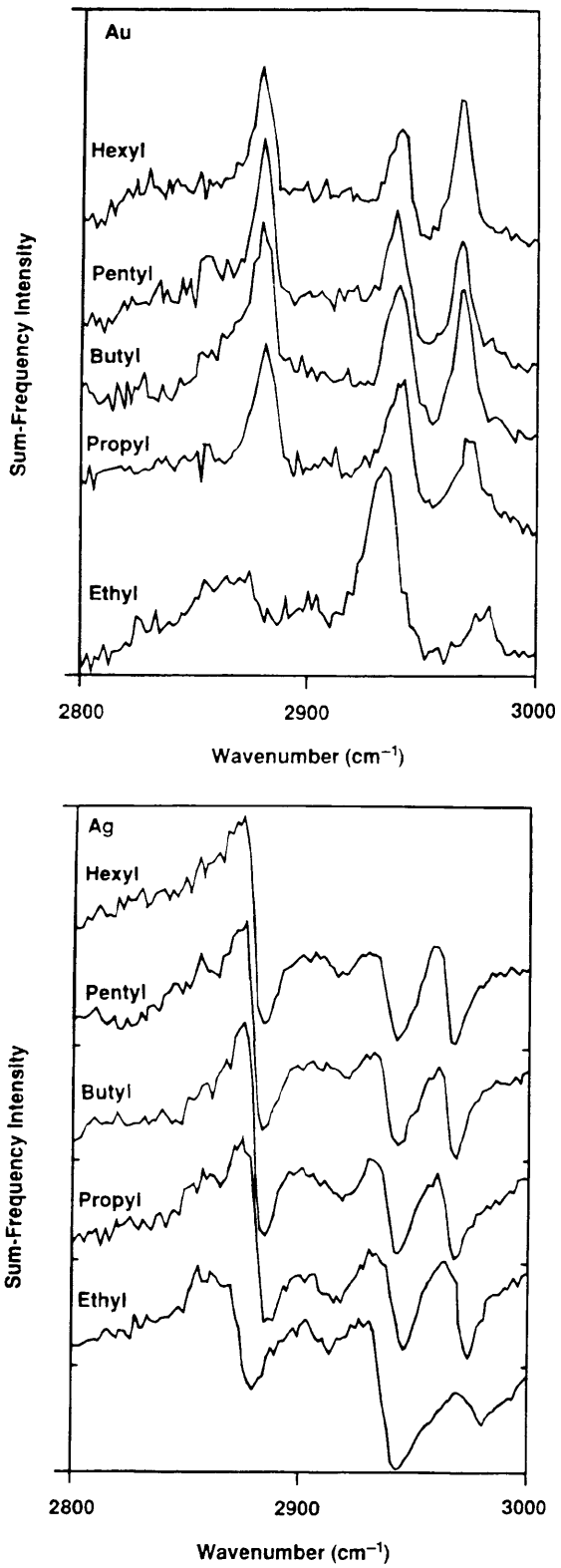

Figure 10. Sum-frequency spectra of monolayers of $HS(CH_2)_{16}OR$ on gold (upper panel) and silver (lower panel). The spectra have been offset vertically for clarity, and the nonresonant background has been subtracted from the spectra of monolayers on gold. Peak assignments are given in the caption to Figure 9.

Wetting. SAMs derived from $HS(CH_2)_nOR$ provide a system

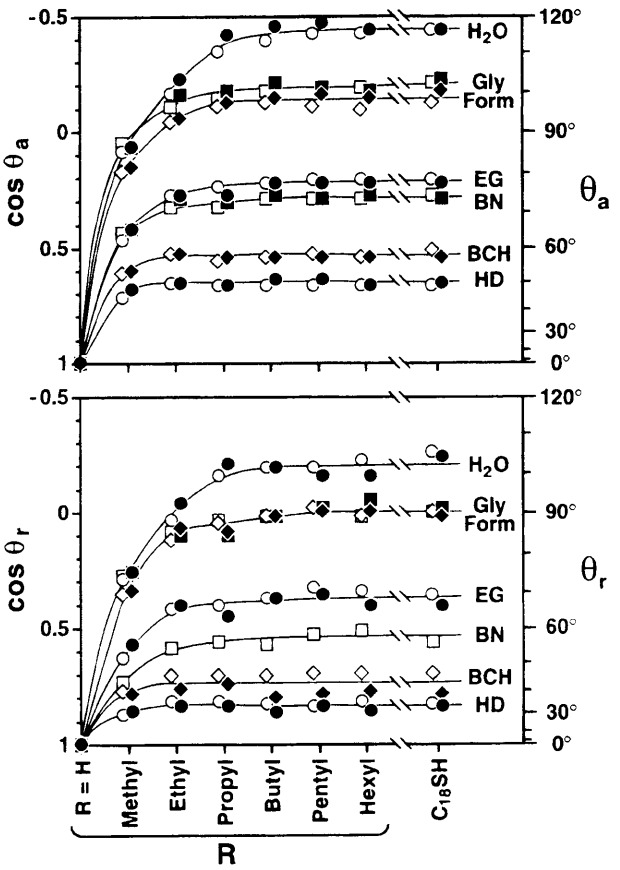

Figure 11. Advancing and receding contact angles (θ_a and θ_r, respectively) of various liquids on monolayers of $HS(CH_2)_{16}OR$ adsorbed on gold and silver (open and filled symbols, respectively). Reference contact angles are provided in the plot for an unsubstituted SAM derived from n-$C_{18}H_{37}SH$ on the two metals. Contacting liquids are water (circles), glycerol (squares, Gly), formamide (diamonds, Form), ethylene glycol (circles, EG), α-bromonaphthalene (squares, BN), bicyclohexyl (diamonds, BCH), and hexadecane (circles, HD). The lines are provided as guides to the eye. Symbols have been slightly offset horizontally for clarity. Errors in θ_a and θ_r are taken to be ±2°. Receding contact angles of BN on silver have been omitted from the figure as they were ~10° lower than those obtained on gold (Tables 1 and 2); the difference may be due to reaction between silver and the probe liquid.

for examining the sensitivity of wetting measurements to the presence of a submerged polar substituent as it is increasingly screened from a contacting external phase by a thin nonpolar hydrocarbon layer (Figure 1). For a common R group, we obtained lower advancing and receding contact angles (θ_a and θ_r, respectively) for SAMS that were derived from HS $(CH_2)_{11}OR$ (on average, by ~5°) than on those derived from $HS(CH_2)_{16}OR$ (for R = methyl to propyl). As SAMs derived from n-hexadecanethiol (and longer n-alkanethiols) on gold and silver are more highly organized than those derived from n-undecanethiol (and shorter n-alkanethiols),[4] the lower contact angles on SAMs derived from $HS(CH_2)_{11}OR$ may reflect a similar chain length influence in the ether system. For this reason, we focused our examination on the wetting properties of the ether-containing SAMs having the longer polymethylene tether.

Figure 11 displays the static advancing and receding contact angles of water, glycerol (Gly), ethylene glycol (EG), formamide (Form), α-bromonaphthalene (BN), bicyclohexyl (BCH), and hexadecane (HD) on SAMs derived from $HS(CH_2)_{16}OR$ on gold and silver surfaces (see also Tables 1 and 2). The liquids were chosen for their moderately high surface tensions and for the differences that exist in their polar and dispersive natures (Table 5).[42] While these liquids wet surfaces exposing CH_2OH groups

TABLE 5: Surface Tensions (γ_L) and Their Dispersive (d) and Polar (p) Components for Various Probe Liquids (mN/m)[a]

liquid	γ_L	γ_L^d	γ_L^p
n-hexadecane	26.7	26.7	0.0
bicyclohexyl	32.4	32.4	0.0
α-bromonaphthalene	43.9	42.3	1.6
ethylene glycol	48.1	17.5	30.6
formamide	58.3	18.1	40.2
glycerol	63.2	20.5	42.7
water	72.0	10.8	61.2

[a] Values taken from ref 43.

(θ_a < 15°), SAMs containing the ether functionalities exhibited wetting properties by these liquids that closely resembled those obtained on unsubstituted n-alkanethiolate SAMs. Of the ethers, the methoxy-terminated SAMs exhibited the lowest contact angles with these liquids. As the alkyl substituent increased in length, the contact angles asymptotically approached the values obtained on n-alkanethiolate SAMs, suggesting that the length scales of interaction between those probe liquids and the submerged polar substituent was on the order of less than an extended hexyl unit. We observed no chain length sensitivities (i.e. odd–even alternations) in the contact angles of the probe liquids on either substrate.

For quantification of the level of interaction further, Figure 12 compares the wetting data for these liquids on SAMs containing the methoxy, ethoxy, and propoxy substituents with the surface tension (γ_L) and the polar component of the surface tension (γ_L^p) for these probe liquids. We have normalized the wetting data so that Figure 12 illustrates the effectiveness of a tail group to screen the interaction between the ether oxygen atom and a probe liquid (i.e., to have wetting properties less like surfaces exposing CH_2OH groups (y-axis = 0) and more like hydrocarbon surfaces (y-axis = 1)). The data in Figure 12a suggest a rough correlation with surface tension whereby liquids with higher surface tensions are less screened by the alkoxy group. For the ethyl and propyl ethers, the wetting properties of the probe liquids fell into two categories: liquids with the lowest surface tensions (γ_L < 45 dyn/cm) had values of 1 in Figure 12a, and liquids with higher surface tensions had values <1. As surface tensions combine factors from both dispersive and polar interactions (Table 5),[43] we examined what relationships exist between these individual contributors (γ_L^d and γ_L^p, respectively) and their sensitivity to the ether group. Figure 12b plots the screening abilities of the alkoxy groups for the various probe liquids as a function of γ_L^p. In general, the data shown in Figure 12b suggest that the wetting properties of polar liquids are more affected by the presence of the submerged polar functionality than are nonpolar liquids. A related plot of the wetting data against γ_L^d exhibited no obvious trend.

In Figure 12b, the nonpolar liquids—HD, BCH, and BN ($\gamma_L^p \approx 0$)—are sensitive to the incorporated heteroatom only for the case of the methyl ether. The scatter in Figure 12b around $\gamma_L^p \approx 0$ for the methoxy terminus suggests that differences in the dispersive nature of these liquids may affect their wetting properties on this particular surface. On the other ether-containing SAMs (ethyl and longer), the wetting properties of these liquids are the same as those seen on n-alkanethiolate SAMs and suggest that the depth being probed by these liquids is less than the length of an ethyl unit (~2 Å). Further, the outermost structure of the ether-containing SAMs (R = ethyl to hexyl) on this dimension must be similar in nonpolar environments to those of unsubstituted SAMs.

The wetting properties of the polar liquids ($\gamma_L^p > 0$) on these surfaces exhibit a higher sensitivity to the incorporated oxygen

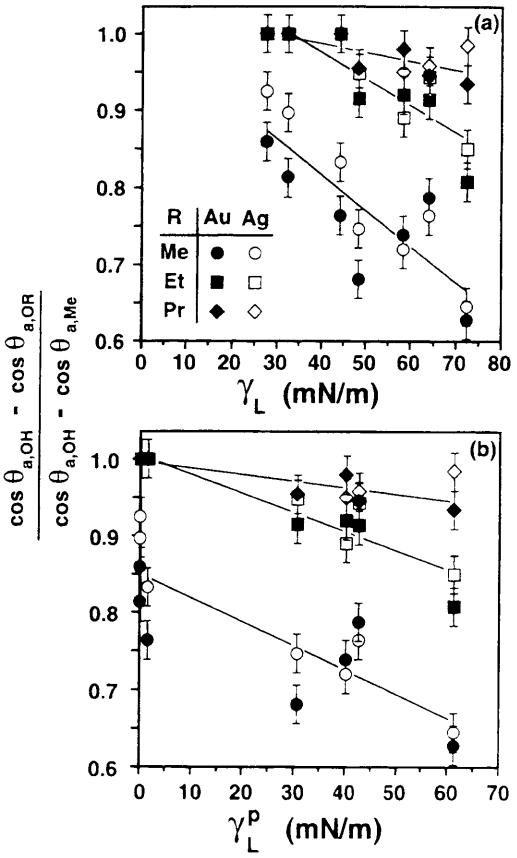

Figure 12. Effect of surface tension and liquid polarity on the wetting properties of SAMs derived from $HS(CH_2)_{16}OR$ on gold and silver. γ_L^P is the polar component of the surface tension (γ_L) of a liquid. The y-axis is a normalized expression that is related to the ratio of two interfacial free energies: here, $\theta_{a,TailGroup}$ is the advancing contact angle of a liquid on a SAM derived from $HS(CH_2)_{16}TailGroup$; $\theta_{a,OH}$ was taken to equal 0° for all liquids, and advancing contact angles measured on SAMs derived from n-$C_{18}H_{37}SH$ were used for $\theta_{a,Me}$. The y-axis is a measure of the influence of the ether oxygen on the wetting properties of a liquid, with lower values reflecting larger relative deviations from the wetting properties obtained on SAMs lacking the ether oxygen. Data for the butyl, pentyl, and hexyl ethers would appear in the plots as points scattered about $y = 1.0$ for all values of γ_L and γ_L^P. Solid lines are least squares fits to the data and are provided solely as guides to the eye. Errors in θ_a are taken to be ±2°.

atom than do the nonpolar liquids. As shown in Figure 11, the wetting properties are different for the methyl, ethyl, and propyl ethers and contrast significantly those of unsubstituted SAMs. These differences suggest that the polar liquids sense the presence of the submerged functional group over depths of approximately a propyl unit. The sensing mechanism is likely one of proximity and does not reflect the penetration of the SAM by the contacting liquid. We expect that as the structures on gold are more canted than those on silver, solvent penetration into the SAMs on gold should be easier than on silver. As a result, the SAMs on gold should exhibit increased contact angle hysteresis and lower values of θ_a if penetration if occurring. Within error, the contact angle hysteresis and the values of θ_a are the same on the two metals. The wetting properties of the butyl, pentyl, and hexyl ethers by the polar liquids are the same as on unsubstituted n-alkanethiolate SAMs. This observation suggests that the wetting measurements by these liquids probe a depth less than the length of an extended butyl unit (~5 Å) and that the outermost surfaces of the ether-containing SAMs (R = butyl to hexyl) in contact with these liquids are similar to those of pure alkyl SAMs under these conditions.

The important structural conclusions that emerge from the wetting results are that the SAMs are oriented, they are densely

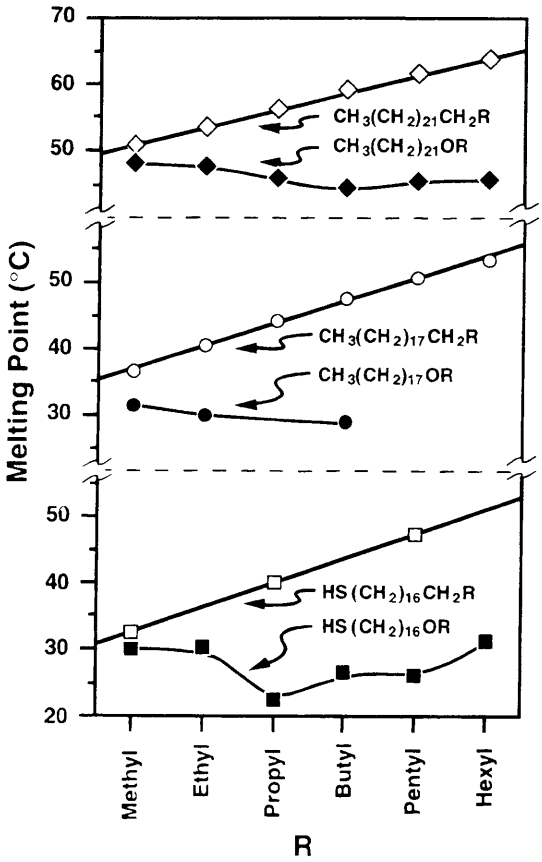

Figure 13. Melting points of various unsymmetrical di-n-alkyl ethers and isometric n-alkanes. The melting point of $CH_3(CH_2)_{17}O(CH_2)_7$-CH_3 is 35–36 °C;[44] the corresponding alkane $CH_3(CH_2)_{25}CH_3$ melts at 59.0–59.1 °C.[44] Lines are provided as guides to the eye.

packed and, for the butyl, pentyl, and hexyl ethers, present structures to condensed media that are energetically (and presumably structurally) similar to those of n-alkanethiolate SAMs on the respective metals in these liquids. This latter conclusion also appears to extend to the ethyl and propyl ethers when the contacting phase is relatively nonpolar.

Extension to the Solid State

In the above studies, we frequently compared the properties and spectral characteristics of the ω-alkoxy-n-alkanethiolate SAMs on silver and gold with those of n-alkanethiolates on the corresponding metal. Many of the spectroscopic-based conclusions regarding the structure of the n-alkanethiolate SAMs on these metals are based on the solid-state structures of related compounds, primarily n-alkanes and n-alkyl disulfides. Ideally, we should compare the ω-alkoxy-n-alkanethiolate SAMs with the structures of crystalline long chain di-n-alkyl ethers; however, these materials are difficult to crystallize, and no X-ray crystal structures are available. We have used melting points and XPS to provide qualitative information regarding this class of molecules. (High resolution XP spectra are included in the supplementary materials.)

Melting Points. Melting point provides an easily measured, albeit qualitative, meter of order. In Figure 13, we plot the melting points for a series of n-alkyl ethers and for isometric n-alkanes and n-alkanethiols.[44] For these structures, the replacement of a CH_2 unit by an oxygen atom depresses the melting point of the materials. More importantly, the addition of methylene units to the R group has essentially no effect on the melting point of the ether materials over the range R = methyl to hexyl. In contrast, the melting points of the non-ether containing materials exhibit a consistent increase of ~4°/CH_2

in R over this range. These two trends produce the result that hexyl derivatives exhibit the largest differences in melting point in the figure for isometric molecules. Qualitatively, these observations suggest that the ether systems (at least for R = methyl to butyl) are inherently more disordered than their alkyl analogues. The SAMs offer an interesting contrast in this regard. The strong structural patterns established by the head group bonding are without a real counterpart in the solid-state organization of organic materials. In SAMs, the lattice is fixed and the increased "flexibility" of a segment cannot induce a structural phase transition in the same way as might be occurring in a bulk phase. We expect, therefore, that the perturbation afforded by the ether—namely, a shallow preference for gauche conformations—should be much more weakly expressed in the SAMs. The data appear to support this latter notion and provide a rationale for how SAMs can be exploited to explore atypical organizational patterns of organic molecules.

Discussion

These data establish that the SAMs formed by ω-alkoxy-*n*-alkanethiols on both silver and gold are approximately isostructural with those derived from *n*-alkanethiols. The differences that are noted are largely ones of chain-length-dependent reconstructions of the regions of the SAM lying above the ether oxygen atom. The structure on each metal is one involving a canted, nearly all-trans chain (Figure 7); we estimate the cants are $<12°$ for SAMs on silver and $>25°$ for SAMs on gold (Figure 1). The rotation of the chain in each SAM differs and accords with the previously defined structures of the *n*-alkanethiolate SAMs on these metals.[9,23]

The methyl ether surface on both metals is extensively reconstructed. The infrared data clearly reveal that relaxations at this surface completely obscures the expected odd−even fluctuations in the methyl mode intensities on gold when the length of the underlying polymethylene chain (n) is varied. The methyl mode intensities on both silver and gold are similar despite the different canted phases of the polymethylene chains in these SAMS. The similarity of the methyl mode intensities under these different conditions points to a surface having a common structure free from the influences of the values or signs of α or β. This conclusion is also supported by the SFS results where it was found that the intensity of the methyl modes of the ethers on gold were markedly weaker than in their simple *n*-alkanethiol analogues. This decrease in intensity probably arises from a greater orientational disorder in the terminal methyl groups for the shorter length R groups. As expected, this effect was less pronounced on silver. On both metals, the methoxy derivatives were the only ether-containing SAMs that exhibited wetting properties by the nonpolar liquids that were different from the wetting properties of SAMs derived from *n*-alkanethiols (Figure 12). This observation suggests that the methoxy surfaces, when contacted with a nonpolar liquid phase, differ chemically and/or structurally from the other alkoxy surfaces. This conclusion is compatible with the spectroscopic results on this surface where the contacting phase—air or vacuum—was also a nonpolar medium.

The structures of the SAMs are distinguished by the aforementioned chain length sensitivity of the surface reconstruction. The rather large relaxations inferred for the surface of the methyl ether SAMs are nearly absent in the ethers with an R group longer than a propyl unit. It has been noted that the oxygen atom induces a slight preference for a gauche conformation in a hydrocarbon chain.[27] In a SAM, the associated loss of crystalline packing in the region above the oxygen atom would come at an energetic cost. If we assume the magnitude of this energy is given approximately by the group constituent heat of fusion per methylene unit (that is to say that the chain melts above the heteroatom), we can estimate the compensating energy term in this system. For chains of the order of propyl and butyl groups, this factor would contribute ~0.2−0.6 kcal/mol at 300 K. This value is roughly of the order of the energy assumed above for the favoring of gauche conformations at the OCC bonds.[27] Thus, for R groups longer than propyl or butyl groups, the preference for gauche conformations about the ether oxygen atom becomes energetically unfavorable, and the SAMs on both silver and gold are structurally similar to their *n*-alkanethiolate analogues. The variable temperature infrared data for the hexyl ether derivative on gold (Figure 8) also suggest that the lowest energy structure of these SAMs likely involves a multichain unit cell. The quantitative aspects of the spectral data are such that the four-chain unit cell indicated by diffraction studies of *n*-alkanethiolate SAMs on gold[22] may be present here as well.

In every respect, then, the larger organization of the SAMs, save the quantitative differences in the surface reconstructions, follows closely from the alkane to the ether systems. This implicitly establishes that the sulfur lattice on which these SAMs order is also very (if not completely) similar. We believe that the ω-alkoxy-*n*-alkanethiolate SAMs on both silver and gold adopt hexagonal structures akin to those of the *n*-alkanethiolate SAMs; the structure on gold is most likely a commensurate $(\sqrt{3} \times \sqrt{3})R30°$ overlayer, while the structure on silver is an incommensurate overlayer as judged from the magnitude of the chain cants. There is nothing, then, in the character of the ether substituent that can alter these bonding arrangements via chain−chain interaction energies.

One of the more intriguing issues raised by the current data is the influence of both temperature and contacting solvent on the organization of the surface of the SAM. We found, for example, that relatively short chains—on the order of a propyl or butyl group—can undo the reconstructions favored by the ether oxygen atom. This observation is not likely to be a condition-independent result, as the energetics at an interface with air are not the same as those with a liquid. Solvent interactions are expected to derive surface reorganizations, and the degree to which these ensue for any given R chain length would also depend on the temperature. The wetting data reveal that the screening of the heteroatom from the contacting phase depends very sensitively on the nature of the solvent used (Figure 12). The more polar the contacting liquid is, the more deeply is the heteroatom sensed. This dependence on polarity may reflect some subtle difference in the mechanism(s) of the interaction (see above), but the contributions of concomitant reorganizations cannot be excluded. This latter effect is very strongly implicated by published SFS studies performed with these SAMs in contact with liquids.[12] These SFS studies and the wetting data presented here demonstrate that an R group as short as a butyl unit is sufficient at room temperature to prevent interactions between polar liquids (such as water) and the "buried" polar oxygen atom, so that the SAM behaves like an unsubstituted *n*-alkanethiolate SAM in all respects.

The conclusion that the effect of the incorporated ether oxygen atom on the structure of the SAM is overcome by a butyl group (and by a propyl group when the SAM is contacted with a nonpolar phase) contrasts with conclusions from other examinations of substituted SAMs. Limited data exist for direct comparison as most studies have used longer tail groups (*n*-C_9H_{19},[45] *n*-$C_{11}H_{23}$,[25] *n*-$C_{12}H_{25}$,[24,45,46] and *n*-$C_{16,17}H_{33,35}$[13]) to compensate for the incorporated moiety. Ulman et al. have incorporated sulfones within alkanethiolate SAMs[25] and phenyl groups within alkylsiloxane[45,46] and alkanethiolate SAMs[24] and examined the effect of these substitutions on the structure and

properties of the SAMs. In these studies, they observed that the wetting properties of the SAMs by hexadecane and water were lower than those on the corresponding unsubstituted SAMs and that the methyl modes exhibited broadened IR absorption peaks. They concluded that a C_{12} chain was required above the incorporated moiety to mask its presence. In the present work, the substitution of an oxygen atom for a methylene unit imposes less steric demands than these other incorporated moieties. This difference—that the incorporated unit is commensurate in size with the polymethylene chains that comprise the SAM—could well account for the difference that a C_4 unit (instead of a C_{12} unit) is sufficient to mask the presence of the underlying polar substituent.

The structural perturbations to the SAMs by the incorporated oxygen atom appear less severe than might be expected from the properties and structural simulations of alkyl ethers. We believe that the difference results from a strong ordering element in the SAMs, the metal—thiolate interaction, that provides a common anchoring point for the ether-containing materials. As such, the ordered framework of SAMs appears to provide a convenient and flexible system for examining some of the structural aspects of poorly ordered solid—state materials.

Experimental Section

Materials. Single crystal silicon wafers oriented in the [100] direction were obtained from Silicon Sense (Nashua, NH) or Virginia Semiconductors. Wafers used for infrared spectroscopy were 50 mm in diameter and ~250 μm thick; wetting and XPS studies used 1 × 3 cm^2 slides cut from Si(100) wafers that were 100 mm in diameter and ~500 μm thick. The purities of the gold (Materials Research Corp. or Johnson Matthey) and silver (Aldrich or Johnson Matthey) used for evaporations were 99.99% or higher. Absolute ethanol (Quantum Chemical or James Burroughs) used for adsorption solutions was deoxygenated by bubbling N_2 for 30 min prior to use. Octadecanethiol (Aldrich) was recrystallized prior to use. Prepurified Ar (>99.998%, <5 ppm O_2) was obtained from Med-tech. 16-Mercapto-1-hexadecanol and *n*-octadecanethiol-d_3 were available from previous studies.[8,23] Syntheses and spectral properties of the ω-alkoxy-*n*-alkanethiols and 1-alkoxydocosanes are given in the supplementary material to this paper.

Sample Preparation. The substrates were prepared by evaporation of silver or gold (1000—2000 Å) onto silicon wafers primed with 100—200 Å of chromium or titanium as an adhesion layer; silver substrates prepared for wetting and XPS studies were onto precut 1 × 3 cm^2 slides of silicon. Metals were evaporated at a rate of ~5 Å/s in either a cryogenically-pumped electron beam chamber (base pressure ~ 8 × 10^{-8} Torr) or a thermal evaporator evacuated with a diffusion pump and liquid nitrogen trap (base pressure = 1 × 10^{-6} Torr); the properties of the SAMs were not sensitive to the evaporator used. The evaporations produce highly reflective, polycrystalline metal films that are heavily (111) textured. For evaporations of silver, the chamber was back-filled with prepurified argon immediately following evaporation, and the substrates transferred under a flow of argon to adsorption solutions. The back-fill and transfer procedures took at most 7 min. SAMs were prepared by 12—48-h exposure of the substrates to 1 mM deoxygenated ethanolic solutions of the thiols in single-use scintillation vials (20 mL).[8,9] Samples for IR were prepared in a related manner on 50 mm Si(100) wafers and functionalized in Petri dishes. Slides were removed from the solutions, washed with ethanol, and blown dry with N_2 prior to characterization.

Ellipsometry. Ellipsometric thicknesses were determined for SAMs on gold as has been described prevously using a refractive index of 1.45.[4,5] This value was used for consistency with previous studies and as the difference in refractive indices for alkyl ethers and their isometric *n*-alkanes is small ($\Delta < 0.01$).[47] The ellipsometric constants were measured at three different locations on each slide; thicknesses give in Table 1 are the average of at least three slides from at least two independent preparations.

Contact Angles. Contact angles were measured using a Ramé-Hart goniometer under ambient conditions on both sides of static drops that had been advanced or receded over the surface using an Electra-Pipette dispenser (Matrix Technologies, Lowell, MA) at ~ 1 μL/s; the tip of the pipet remained in the drop during the measurements. Drops were always applied to previously uncharacterized sections of the slide. Data presented in the tables and figures are the average of measurements of at least three drops.

X-ray Photoelectron Spectroscopy (XPS). Spectra were obtained using a Surface Science Laboratories X-100 X-ray photoelectron spectrometer. The spectrometer employs monochromatized Al Kα X-rays and a hemispherical multichannel detector. Spectra of the monolayers were referenced to Au($4f_{7/2}$) = 84.00 eV and either Ag($3d_{5/2}$) = 368.7 eV or C(1s) = 284.9 eV. Spectra of the alkyl docosyl ethers were obtained using a 2-eV flood gun to minimize charging, and the C(1s) photoelectron peak corresponding to bulk hydrocarbon was referenced to 284.91 eV—the position determined for the C(1s) peak with the SAMs adsorbed on gold. High resolution spectra (50 scans, ~2 min/spectrum) were obtained at a pass energy of 25 eV and a spot size of 300 μm. Attenuation data for the underlying substrates were obtained at a pass energy of 100 eV and a spot size of 1000 μm (1 scan, ~2 min/spectrum); each sample was individually focused and run in random order. These data provided reference substrate intensities that were used to scale the high resolution O(1s) peak areas for the various SAMs (Figure 3c).

Infrared Sectroscopy. The methods used to acquire RAIRS data have been described in detail elsewhere.[36] Room temperature spectra were taken using an *n*-octadecanethiolate-d_{37} SAM on the metal of interest as reference. Low temperature data were acquired in a standard reflection geometry with *f*/14 optics at an ~82° angle of incidence in a ultrahigh vacuum cell with a base pressure of <6 × 10^{-10} Torr. Cooling was provided by a regulated liquid N_2 cold finger; the sample was held to within 2 K of the reported temperature. The data were collected as difference spectra (− log $I_T/300K$) and converted to absolute spectra using the authentic absorbance spectrum of the sample at 300 K.

Sum-Frequency Generation Spectroscopy (SFS). Tunable infrared laser radiation (~4 ns, ~600 μJ/pulse, 10 Hz) was generated by difference-frequency mixing in a $LiNbO_3$ crystal of the Nd:YAG fundamental with the output of the Nd:YAG-pumped tunable dye laser. The visible radiation (6 ns, 1—1.5 mJ/pulse) was obtained by frequency doubling the Nd:YAG fundamental. The angles of incidence were 55° at 532 nm and 60° at 2800—3000 cm^{-1} in a counter-propagating geometry. Light emitted at the sum frequency (in a direction determined by the **k** vector matching at the surface) was filtered and detected by a photomultiplier tube. Each spectrum took ~45 min to acquire.

Acknowledgment. We are grateful to R. N. Ward and T. H. Ong for their assistance in obtaining the SF spectra.

Supplementary Material Available: Text, with accompanying references, of syntheses and characterization of ω-alkoxy-*n*-alkanethiols and 1-alkoxy-*n*-docosanes and figures of high resolution XPS data of the C(1s) and O(1s) spectral regions or polycrystalline 1-alkoxy-*n*-docosanes as solid state samples and

for ω-alkoxy-*n*-hexadecanethiolate SAMs on gold and silver and RAIRS spectra of $HS(CH_2)_{16}O(CH_2)_3CH_3$ and $HS(CH_2)_{16}O(CD_2)_3CD_3$ on gold and silver (13 pages). Ordering information is given on any current masthead page.

References and Notes

(1) This work was supported in part by the Office of Naval Research and the Advanced Research Projects Agency. C.D.B. acknowledges support from Unilever Research and SERC. XPS spectra were obtained using instrumental facilities purchased under the DARPA/URI program and maintained by the Harvard University Materials Research Laboratory. R.G.N. acknowledges support from the Department of Energy through the UIUC Materials Research Laboratory (Grant DEFG02-91ER45439).

(2) Early results of this study have been communicated: Bain, C. D.; Whitesides, G. M. *J. Am. Chem. Soc.* **1988**, *110*, 5897−5898.

(3) Nuzzo, R. G.; Allara, D. L. *J. Am. Chem. Soc.* **1983**, *105*, 4481−4483.

(4) Porter, M. D.; Bright, T. B.; Allara, D. L.; Chidsey, C. E. D. *J. Am. Chem. Soc.* **1987**, *109*, 3559−3568.

(5) Bain, C. D.; Troughton, E. B.; Tao, Y.-T.; Evall, J.; Whitesides, G. M.; Nuzzo, R. G. *J. Am. Chem. Soc.* **1989**, *111*, 321−335.

(6) For reviews of *n*-alkanethiolate SAMs on gold, see: Bain, C. D.; Whitesides, G. M. *Angew. Chem., Int. Ed. Engl.* **1989**, *101*, 522−528. Whitesides, G. M.; Laibinis, P. E. *Langmuir* **1990**, *6*, 87−96. Dubois, L. H.; Nuzzo, R. G. *Annu. Rev. Phys. Chem.* **1992**, *43*, 437−463.

(7) Walzcak, M. M.; Chung, C.; Stole, S. M.; Widrig, C. A.; Porter, M. D. *J. Am. Chem. Soc.* **1991**, *113*, 2370−2378.

(8) Laibinis, P. E.; Whitesides, G. M.; Allara, D. L.; Tao, Y.-T.; Parikh, A. N.; Nuzzo, R. G. *J. Am. Chem. Soc.* **1991**, *113*, 7152−7167.

(9) Laibinis, P. E.; Whitesides, G. M. *J. Am. Chem. Soc.* **1992**, *114*, 1990−1995.

(10) Bain, C. D.; Whitesides, G. M. *J. Am. Chem. Soc.* **1988**, *110*, 6560−6561. Bain, C. D.; Whitesides, G. M. *Langmuir* **1989**, *5*, 1370−1378. Dubois, L. H.; Zegarski, B. R.; Nuzzo, R. G. *J. Am. Chem. Soc.* **1990**, *112*, 570−579. Ulman, A.; Evans, S. D.; Shnidman, Y.; Sharma, R.; Eilers, J. E. *Adv. Colloid Interface Sci.* **1992**, *39*, 175−224. Ulman, A.; Evans, S. D.; Sharma, R. *Thin Solid Films* **1992**, *210*, 810−814. Nuzzo, R. G.; Zegarski, B. R.; Korenic, E. M.; Dubois, L. H. *J. Phys. Chem.* **1992**, *96*, 1355−1361.

(11) Ong, T. H.; Ward, R. N.; Davies, P. B.; Bain, C. D. *J. Am. Chem. Soc.* **1992**, *114*, 6243−6245.

(12) Ong, T. H.; Davies, P. B.; Bain, C. D *Langmuir* **1993**, *9*, 1836−1845.

(13) Chang, S.-C.; Chao, I.; Tao, Y.-T. *J. Am. Chem. Soc.* **1994**, *116*, 6792−6805.

(14) Pale-Grosdemange, C.; Simon, E. S.; Prime, K. L.; Whitesides, G. M. *J. Am. Chem. Soc.* **1991**, *113*, 12−20. Häussling, L.; Michel, B.; Ringsdorf, H.; Rohrer, H. *Angew. Chem., Int. Ed. Engl.* **1991**, *30*, 569−572. Prime, K. L.; Whitesides, G. M. *Science (Washington, DC)* **1991**, *252*, 1164−1167. Czanderna, A. W.; King, D. E.; Spaulding, D. *J. Vac. Sci. Technol. A* **1991**, *9*, 2607−2613. Smith, E. L.; Alves, C. A.; Anderegg, J. W.; Porter, M. D.; Siperko. L. M. *Langmuir* **1992**, *8*, 2707−2714. Stenger, D. A.; Georger, J. H.; Dulcey, C. S.; Hickman, J. J.; Rudolph, A. S.; Nielsen, T. B.; McCort, S. M.; Calvert, J. M. *J. Am. Chem. Soc.* **1992**, *114*, 8435−8442. Jung, D. R.; King, D. E.; Czanderna, A. W. *Appl. Surf. Sci.* **1993**, *70/71*, 127−132. Jung, D. R.; King, D. E.; Czanderna, A. W. *J. Vac. Sci. Technol. A* **1993**, *11*, 2382−2386. López, G. O.; Albers, M. W.; Schreiber, S. L.; Carroll, R.; Peralta, E.; Whitesides, G. M. *J. Am. Chem. Soc.* **1993**, *115*, 5877−5878. DiMilla, P. A.; Folkers, J. P.; Biebuyck, H. A.; Härter, R.; López, G. P.; Whitesides, G. M. *J. Am. Chem. Soc.* **1994**, *116*, 2225−2226.

(15) Frostman, L. M.; Bader, M. M.; Ward, M. D. *Langmuir* **1994**, *10*, 576−582.

(16) Chidsey, C. E. D.; Loiacono, D. N. *Langmuir* **1990**, *6*, 682−691. Chidsey, C. E. D. *Science (Washington, DC)* **1991**, *251*, 919−922. Becka, A. M.; Miller, C. J. *J. Phys. Chem.* **1992**, *96*, 2657−2668. Becka, A. M.; Miller, C. J. *J. Phys. Chem.* **1993**, *97*, 6233−6239.

(17) Laibinis, P. E.; Graham, R. L.; Biebuyck, H. A.; Whitesides, G. M. *Science (Washington, DC)* **1991**, *254*, 981−983. Graham, R. L.; Bain, C. D.; Biebuyck, H. A.; Laibinis, P. E.; Whitesides, G. M. *J. Phys. Chem.* **1993**, *97*, 9456−9464.

(18) Nuzzo, R. G.; Korenic, E. M.; Dubois, L. H. *J. Chem. Phys.* **1990**, *93*, 767−773.

(19) Strong, L.; Whitesides, G. M. *Langmuir* **1988**, *4*, 546−558.

(20) Bryant, M. A.; Pemberton, J. E. *J. Am. Chem. Soc.* **1991**, *113*, 8284−8293.

(21) Bryant, M. A.; Pemberton, J. E. *J. Am. Chem. Soc.* **1991**, *113*, 3629−3637.

(22) Camillone, N., III; Chidsey, C. E. D.; Liu, G.-Y.; Putvinski, T. M.; Scoles, G. *J. Chem. Phys.* **1991**, *94*, 8493−8502. Fenter, P.; Eisenberger, P.; Li, J.; Camillone, N., III; Bernasek, S.; Scoles, G.; Ramanarayanan, T. A.; Liang, K. S. *Langmuir* **1991**, *7*, 2013−2016. Dubois, L. H.; Zegarski, B. R.; Nuzzo, R. G. *J. Chem. Phys.* **1993**, *98*, 678−688. Camillone, N., III; Chidsey, C. E. D.; Eisenberger, P.; Fenter, P.; Li, J.; Liang, K. S.; Liu, G.-Y.; Scoles, G. *J. Chem. Phys.* **1993**, *99*, 744−747. Fenter, P.; Eisenberger, P.; Liang, K. S. *Phys. Rev. Lett.* **1993**, *70*, 2447−2450.

(23) Nuzzo, R. G.; Dubois, L. H.; Allara, D. L. *J. Am. Chem. Soc.* **1990**, *112*, 558−569.

(24) Evans, S. D.; Urankar, E.; Ulman, A.; Ferris, N. *J. Am. Chem. Soc.* **1991**, *113*, 4121−4131.

(25) Evans, S. D.; Goppert-Berarducci, K. E.; Urankar, E.; Gerenser, L. J.; Ulman, A.; Synder, R. G. *Langmuir* **1991**, *7*, 2700−2709.

(26) Popenoe, D. D.; Deinhammer, R. S.; Porter, M. D. *Langmuir* **1992**, *8*, 2521−2530. Batchelder, D. N.; Evans, S. D.; Freeman, T. L.; Haussling, L.; Ringsdorf, H.; Wolf, H. *J. Am. Chem. Soc.* **1994**, *116*, 1050−1053. Yip, C. M.; Ward, M. D. *Langmuir* **1994**, *10*, 549−556.

(27) Miwa, Y.; Machida, K. *J. Am. Chem. Soc.* **1989**, *111*, 7733−7739. and references cited therein.

(28) Folkers, J. P.; Zerkowski, J. A.; Laibinis, P. E.; Seto, C. T.; Whitesides, G. M. In *Supramolecular Architecture in Two and Three Dimensions*; Bein, T., Ed.; ACS Symposium Series No. 499, American Chemical Society: Washington, DC, 1992, pp 10−23.

(29) In these studies, we use polycrystalline films that are predominantly (111) in texture.[8] The structures of these films determined from diffraction studies on single crystalline substrates[19,22] have agreed with the structures determined by vibrational spectroscopies on polycrystalline[4,7,8] and macroscopically roughened surfaces.[20,21]

(30) The cant of the hydrocarbon chain of *n*-alkanethiolate SAMs on gold exhibits no change when the CH_3 group is replaced with tail groups commensurate in size with the polymethylene chain (e.g. X = $CONH_2$, CO_2H, CH_2OH, and CO_2CH_3).[23]

(31) Hautman, J.; Klein, M. L. *J. Chem. Phys.* **1990**, *93*, 767−773.

(32) Folkers, J. P.; Laibinis, P. E.; Whitesides, G. M.; Deutch, J. *J. Phys. Chem.* **1994**, *98*, 563−571.

(33) Laibinis, P. E.; Fox, M. A.; Folkers, J. P.; Whitesides, G. M. *Langmuir* **1991**, *7*, 3167−3173. Folkers, J. P.; Laibinis, P. E.; Whitesides, G. M. *Langmuir* **1992**, *8*, 1330−1341. Laibinis, P. E.; Nuzzo, R. G.; Whitesides, G. M. *J. Phys. Chem.* **1992**, *96*, 5097−5105. Stranick, S. J.; Parikh, A. N.; Tao, Y.-T.; Allara, D. L.; Weiss, J. P. *J. Phys. Chem.* **1994**, *98*, 7636−7646.

(34) Abrahamsson, S.; Larsson, G.; von Sydlow, E. *Acta Crystallogr.* **1960**, *13*, 770−774.

(35) Bain, C. D.; Whitesides, G. M. *J. Phys. Chem.* **1989**, *93*, 1670−1673. Laibinis, P. E.; Bain, C. D.; Whitesides, G. M. *J. Phys. Chem.* **1991**, *95*, 7017−7021.

(36) Allara, D. L.; Nuzzo, R. G. *Langmuir* **1985**, *1*, 52−66. Nuzzo, R. G.; Fusco, F. A.; Allara, D. L. *J. Am. Chem. Soc.* **1987**, *109*, 2358−2367.

(37) Henbest, H. B.; Meakins, G. D.; Nicholls, B.; Wayland, A. A. *J. Chem. Soc.* **1957**, 1462−1464. Allan, A.; McKean, D. C.; Perchard, J.-P.; Josien, M.-L. *Spectrochim. Acta* **1971**, *27A*, 1409−1437.

(38) Bellamy, L. J. *The Infrared Spectra of Complex Molecules*; Chapman & Hall: London, 1980; pp 16−21 and references cited therein.

(39) Eisenthal, K. B. *Annu. Rev. Phys. Chem.* **1992**, *43*, 627−661.

(40) Bain, C. D.; Davies, P. B.; Ong, T. H.; Ward, R. N.; Brown, M. A. *Langmuir* **1991**, *7*, 1563−1566.

(41) Shen, Y. R. *The Principles of Non-Linear Optics*; Wiley: New York, 1984.

(42) Harris, A. L.; Chidsey, C. E. D.; Levinos, N. J.; Loiacono, D. N. *Chem. Phys. Lett.* **1987**, *141*, 350−356.

(43) Panzer, J. *J. Colloid Interface Sci.* **1973**, *44*, 142−161.

(44) *n*-Alkanes: *Beilstein Handbuch der Organischen Chemie*; Springer-Verlag: Berlin, 1972; Band I, pp 553−591. Di-*n*-alkyl ethers $C_{18}OC_1$ and $C_{22}OC_1$: Cook, J. S.; Meakins, R. J. *J. Chem. Phys.* **1959**, *30*, 787−790. $C_{18}OC_2$: Shirley, D. A.; Zeitz, J. R.; Jr. *J. Org. Chem.* **1953**, *18*, 1591−1593. $C_{18}OC_4$ and $C_{18}OC_8$: Shirley, D. A.; Zeitz, J. R., Jr.; Reedy, W. H. *J. Org. Chem.* **1953**, *18*, 378−381. *n*-Alkanethiols: Reference 5.

(45) Tillman, N.; Ulman, A.; Schildkraut, J. S.; Penner, T. L. *J. Am. Chem. Soc.* **1988**, *100*, 6136−6144.

(46) Tillman, N.; Ulman, A.; Elman, J. F. *Langmuir* **1990**, *6*, 1512−1518.

(47) For example, the isometric molecules *n*-nonane and di-*n*-butyl ether have indices of refraction (n_D^{20}) of 1.4054 and 1.3992, respectively: *Handbook of Chemistry and Physics*; Weast, R. C., Ed.; Chemical Rubber Co.: Boca Raton, FL, 1979.

JP942181V